

A new high-resolution seismic catalog for the Southern Apennines (Italy) built through template-matching

G. Diaferia^{1,2}, L. Valoroso¹, L. Improta¹, D. Piccinini³

¹Istituto Nazionale di Geofisica e Vulcanologia, Osservatorio Nazionale Terremoti, Via Vigna Murata 605,
00143, Rome, Italy

²Istituto Nazionale di Geofisica e Vulcanologia, Sezione di Bologna, viale Berti Pichat, 6/2, 40127 Italy

³Istituto Nazionale di Geofisica e Vulcanologia, Sezione di Pisa, Via Cesare Battisti 53, 56125 Pisa, Italy

Key Points:

- template-matching
- high resolution catalog
- Southern Apennines

Corresponding author: G. Diaferia, giovanni.diaferia@ingv.it

Abstract

The incompleteness of earthquake catalogs is a well-known issue caused by our technical limitation in detecting the small- to very small-magnitude seismicity falling near or below the level of background seismic noise. According to the Gutenberg-Richter distribution, small earthquakes represent the majority of the events occurring in a certain area and their detection is key for improving our knowledge of: i) the geometry and kinematics of seismogenic sources; ii) the spatio-temporal characteristics of seismicity, thus leading to better models for seismic hazard. Template-matching (TM) is a well-known and powerful technique based on similarity measure that allows to find earthquakes hidden in the continuous recording, similar to known events (templates). Nowadays, the larger availability of computational resources, allows the application of such technique to regional areas. This work represents the first application of template-matching to Southern Apennines (Italy), using about 4.000 high-quality events as templates and scanning 6-years long continuous recording (2009-2014) at more than 180 stations of the INGV network. About 20.000 new events are found, showing a comparable quality to the template catalog in terms of hypocentral solution, and reaching a decrease of the magnitude of completeness of about one unit. In order to highlight the improved quality of the TM catalog, we report two main examples regarding the Sannio-Matese area, where TM allowed us to unravel relevant details on the spatio-temporal distribution of the local seismicity, providing useful insights for the understanding of the seismic hazard.

Plain Language Summary

The natural and man-made seismic noise commonly surpass the signal of small-size earthquakes that, according to the Gutenberg-Richter distribution, represents the vast majority of the seismic activity. Identifying these hidden events is crucial for gaining a better understanding of fault structures, their location and overall characteristics. A powerful technique for the retrieval of hidden seismicity is template-matching, based on the comparison of known earthquakes with the continuous recording of a network of seismic stations. However, due to the high computational demand, the use of template-matching is usually limited to small areas (e.g. volcanoes) and/or small time periods. In this study, we attempt the first application of template-matching on a regional scale, specifically the Southern Apennines (Italy). We analyze six years of continuous recording from more than 180 stations. Starting from about 4,000 templates, we detected over 20,000 previously

hidden earthquakes with uncertainties on the earthquake location that are low and comparable to those of the initial templates. To demonstrate the potential of this earthquake catalog for future research, we focused on the Sannio-Matese region. For the earthquake sequence in the Matese area occurred between 2013 and 2014, template-matching revealed a consistent level of background seismic before the onset of the sequence, whereas no activity was reported in the official catalog. In the nearby Sannio area, we identified several earthquake clusters at an unusually deep depths, indicating a sudden increase in depth of seismic activity in this area. These observations could significantly contribute to improving the seismic hazard model for the area.

1 Introduction

Despite the theoretical and instrumental advances of the last decades in the field of earthquake seismology, the initiation process of earthquakes remains poorly understood. In general, small magnitude events may precede a mainshock, then followed by a series of aftershocks. In other cases, the seismicity shows a swarm-like behavior, with the earthquake-rate gradually building up and then decreasing towards the long-term background activity. Depending on the case, the earthquakes nucleation and triggering are explained with a variety of processes (or their combination) such as static stress change due to fault slip (Stein, 1999) and dynamic stress change (Felzer & Brodsky, 2006). Fluids can also play a role, causing an increase in hydrostatic pressure (Wei et al., 2015) or aseismic slip due to fluid migration (De Barros et al., 2020). However, our comprehension of the earthquake mechanism is still inadequate and mainly hampered by the technical limitations in the detection of small- to very small-magnitude seismicity. This constitute the vast majority of the whole seismic activity, as predicted by the Gutenberg–Richter law for the frequency-magnitude distribution (Gutenberg & Richter, 1944). However, such small-magnitude events fall below the detectability threshold of conventional short-term/long-term averages algorithms (Allen, 1982) used for real-time earthquakes monitoring and therefore all catalogs at our disposal are inherently incomplete. An effective method which is employed for the detection of hidden seismicity and the improvement of catalog completeness is *template-matching* (TM). Based on cross-correlation measures, the algorithm uses the arrivals of known earthquakes (templates) to identify highly similar, previously undetected events near or below the usual detectability limit (Gibbons & Ringdal, 2006; Shelly et al., 2007; Frank et al., 2014). Template-matching has been widely used across

different scales and for a variety of applications, ranging from the characterization of fluid-induced seismicity (Shelly et al., 2013, 2016), detection of repeating earthquakes (Kato et al., 2012; Chamberlain et al., 2017, 2014; Shelly et al., 2007), and for catalog enhancement at regional scale (Ross et al., 2019). It allows to sharpen our image of the three-dimensional structure of seismogenic faults at depth (Shearer, 2002; Ross et al., 2017), contributing to better seismo-tectonic models and improved estimation of the overall seismic hazard in a certain area. However, large-scale applications of template-matching are still hindered by the high computational burden, mainly due to the massive I/O operation on the continuous recording. Attempts have been made to speed up the computational operation, including the optimization of the cross-correlation algorithm (Beaucé et al., 2018) and/or the parallelization on CPU and GPU infrastructures (Mu et al., 2017; Ross et al., 2019). The aim of this work is to produce a new, enriched earthquake catalog at regional scale, covering the entire Southern Apennines chain (Italy), an area that has been struck by several large earthquakes ($M > 6-7$) in the past 300 years. About 4,000 high-quality events between 2009 and 2014 were used as templates for scanning the continuous waveform recordings of the Istituto Nazionale di Geofisica e Vulcanologia (INGV) seismic network in the same time span. Computations are parallelized on a CPU cluster leading to the detection of about 20,000 new high-quality events, more than 5-fold increase with respect to the initial template catalogue. In the following sections we discuss the characteristics of the starting catalog, the employed template-matching methods and its application. Then we discuss the characteristics of the retrieved seismicity in terms of quality of the hypocentral solutions and its spatio-temporal distribution, in comparison to the starting catalog. Finally, we provide two main examples of application, the first regarding the 2013-2014 Matese sequence, the second focusing on the seismicity distribution in the Sannio area.

2 Method

2.1 Building the template catalog

A high-quality template catalog is a necessary prerequisite for the successful employment of the template-matching technique. In fact, the cross-correlation function highly fluctuates with time-lag, therefore only precise P and S picks of the template's arrivals maximize the chances to detect similar and coherent signals that can be indicative of a new, previously undetected, seismic event. In this work, we decide to focus our effort to

the 2009-2014 time period. Starting from 2009 the INGV seismic network underwent a substantial improvement in terms of quality (i.e. switching to 3-components instruments) and quantity of its sensors, within an upgrading phase initiated in the Southern Apennines as early as 2003 with the CENSIS-INGV project. A total of 183 (mostly) permanent stations (Fig. 1) are deployed in the area of interest, that includes a portion of the Central Apennines, the Irpinia region, the Calabrian Arc and the northwestern sector of the Sicily island. The spacial arrangement of seismic stations is rather inhomogenous, with a lower station density (inter-station distance of about 20-30 km) in areas where the seismic hazard is known to be moderate or low (e.g. the outer sector of the Apennines and the Apulia region).

The Italian Seismic Bulletin (Bollettino Sismico Italiano, BSI) reports about 22.000 events in the study area between 2009 and the end of 2014. Due to the uneven station coverage, varying azimuthal gap and uncertainty assigned to the P and S arrivals, only a portion of such events are worth considering as candidate templates, maximizing the chances to find new detections and maintaining a manageable computational expenditure. For the selection of the candidate templates, we employ the newly released CLASS catalog (Latorre et al., 2022) that consists in all events catalogued in the BSI across the Italian Peninsula from 1981 to 2014, re-located with a probabilistic algorithm and a 3D velocity model (Di Stefano & Ciaccio, 2014). First, we selected all events at a maximum depth of 60 km, having a vertical and horizontal error on the hypocenter location less than two and four km, respectively, with an RMS < 0.8s and an azimuthal gap < 270°. The selection leads to a total of ~9,000 events, with a magnitude of completeness (M_C) of 1.9. We construct an ad-hoc, 1D velocity model (see section 2.3) to be used for determining the hypocenter locations of the known seismicity (and later also for the newly detected events) retaining only the events honoring the criteria (see Table 1) for an high-quality earthquake location. This selection led to a total of 3992 events ($M_C = 2.0$) that are finally employed as templates. As shown in Fig. 4, almost half of the template events refers to the swarm sequence of the Mt. Pollino (Calabria region), started in the second half of 2012 and peaked with a $M_W 5.5$ mainshock (Totaro et al., 2015). The remaining events concentrate around some well known seismogenic structures in the Southern Apennines, such as those reported by the DISS working group (DISS, 2021).

Table 1. Thresholds used for the selection of both templates and new TM-detection.

P picks	≥ 4
S picks	≥ 4
num. stations	≥ 5
h. error	≤ 5 km
v. error	≤ 5 km
RMS	≤ 1 s
az. gap	$\leq 210^\circ$

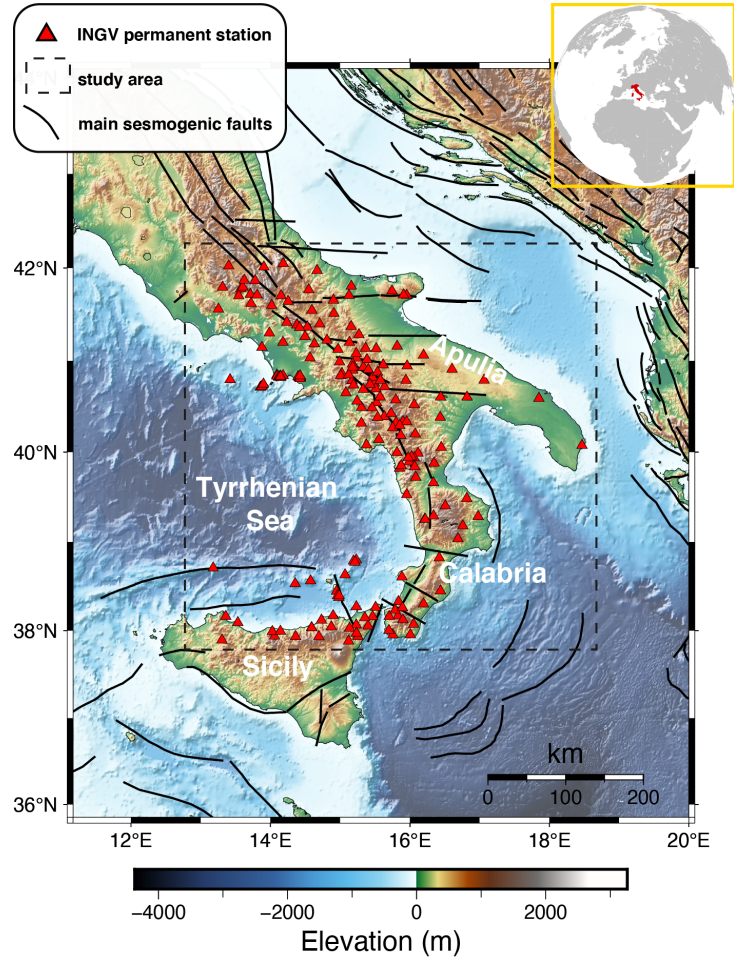


Figure 1. Map of the study area (Southern Apennines, Italy) together with the major seismicogenic faults (associated to events with $M > 5.5$) as reported in the DISS database (<https://doi.org/10.13127/diss3.3.0>) and the +180 permanent stations from the INGV seismic network employed for this study.

2.2 Running the template-matching algorithm

For this study we employed EQcorrscan (Chamberlain et al., 2018), a python-based, open-source code designed for the detection of repeating seismicity through template-matching. The algorithm uses normalized cross-correlation that, in time-domain at the time sample y for a template t with n samples, is:

$$cc(y) = \frac{\sum_{x=0}^n (t(x) - \bar{t})(d(x+y) - \bar{d})}{\sqrt{\sum_{x=0}^n (t(x) - \bar{t})^2 \sum_{x=0}^n (d(x+y) - \bar{d}(y))^2}} \quad (1)$$

with \bar{t} being the mean value of the template signal and \bar{d} being the mean of n -sample long chunk of continuous data. Employing multi-channel data, all the cross-correlation functions of each channel are stacked, taking into account the relative time-delay between channels as in the templates. When the stacked cross-correlation function exceeds a certain threshold this is indicative of a possible new detection, thus the P (only on the vertical component) and S picks (on the horizontal ones) are stored.

Based on testing, we choose a threshold of the stacked cross-correlation function that is 7.5 times the Median Absolute Deviation (MAD), imposing a lower limit of 0.65 for the cross-correlation at each channel. We assign an error to each phase-pick of a newly detected event based on the value of the original pick uncertainty of its template, linearly weighted on the basis of the cross-correlation value. Being $xcorr$ the cross-correlation, e_T the original error on the template pick (commonly 0.1, 0.3, 0.6 or 1 s), we calculate the error on the detection pick e_D as follow:

$$e_D = e_T + e_T(1 - xcorr) \quad (2)$$

Prior to comparison, both templates and continuous waveforms were subjected to identical processing step, consisting in mean/linear trend removal and band-pass filtering between 4 and 15 Hz. By appropriately adjusting the minimum allowable cross-correlation and the length of the template, it can become possible to find an almost exact replication of a know earthquake. In this regard, we opted for a less conservative approach that allowed a wider range of dissimilarity between a new detection and its template, in terms of size, focal mechanism and hypocentral location. For this reason, we also opted for a short template trace (0.5 s from the catalogued P or S pick + a pre-pick of 0.1 s).

In the effort to optimize the amount of continuous data to scan and decrease the computational burden, we initially discarded all stations at more than 40 km from the template event. This decision was based on the assumption that small magnitude events occurring at larger epicentral distances could be hardly detected. However, we finally increased such distance to 80 km, since a test with a subset of 1000 templates showed a 5-fold increase in the total number of new detections with respect to the limit of 40 km that was initially chosen. In fact, by allowing a larger epicentral distance we increase the chance to detect new events with an adequate amount of arrivals, even in area with poor station coverage and high magnitude of completeness, such as those in the external part of the Apennines (where seismic hazard is lower). Given the large amount of data to be scanned, we employed the code on a cluster infrastructure (14 Intel Xeon E5-2680, 2.7 and 2.8 GHz CPUs for a total of 224 cores), with a template-based parallelization where each core run the code for a single template over two years of continuous recording for each chunk. This arrangement allowed an efficient memory usage and a flexible and independent management of each serial job. The total computational expenditure amounted to about $6E10^5$ CPU-hours.

2.3 Data selection, earthquake location and magnitude estimation

The use of template-matching over the six years-long period of continuous recording led to $\sim 10^6$ triggered detections. We selected only those with (see Table 1) i) at least four P and four S picks ii) five of more recording stations, to discard all the events with poor station coverage and an insufficient number of S-wave arrival for an adequate constraint on the hypocentral depth (Husen & Hardebeck, 2011). The earthquake locations have been determined through the probabilistic, non-linear code NonLinLoc (Lomax et al., 2000) using an ad-hoc, 1-D velocity model. This has been constructed by averaging four, 1-D models proposed in the literature (Trionfera et al., 2020; Valoroso et al., 2009; Matrullo et al., 2013; Pastori et al., 2021) and two other 1-D models based on the results of local earthquake tomography and seismic refraction surveys carried out in the Sannio-Irpinia and Basilicata regions (Improta & Corciulo, 2006; Improta et al., 2014, 2017). All models extracted from literature were determined by applying robust inversion schemes (Kissling et al., 1994; Kim et al., 2006) on high-quality travel-time catalogues obtained by dense local networks. To evaluate how the dispersion of the resulting 1-D model may affects the uncertainty of hypocentral parameters, we randomly se-

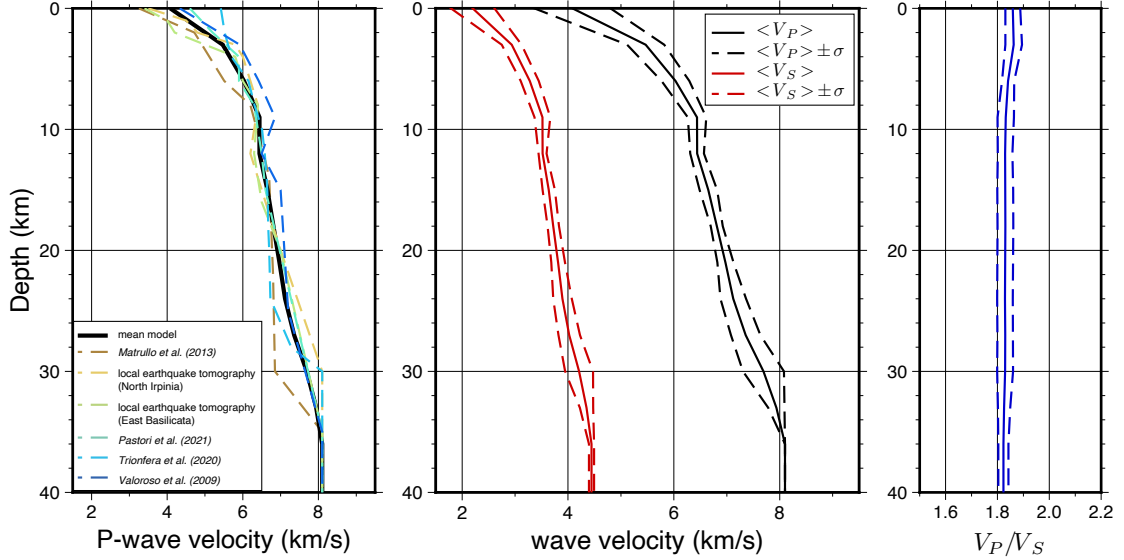


Figure 2. Left panel: velocity models proposed in the literature for different areas within the Southern Apennines and used to build an average, 1-D model (black solid line) for determining earthquake location in this study. Middle panel: average model in terms of P and S wave velocities and their dispersion around the mean value ($\pm\sigma$) at each depth. Right panel: profile V_P/V_S ratio as in the mean model.

lected 1000 events and then located them with 20 randomly sampled models from the mean velocity profile and $\pm 1\sigma$ (see Fig. 2). The majority of events show deviations for the origin time (< 0.1 s) and hypocenter location that are within the uncertainties that typically arise from the errors on the readings of the P and S arrivals. This demonstrates the robustness of our approach when employing a unique, mean and smooth velocity model for the entire study area.

For the estimation of earthquake size we employ a local magnitude (M_L) scale based on the maximum, half peak-to-peak amplitude (A in mm) of the horizontal components. The maximum amplitude is extracted after linear and mean trend removal of the seismic waveforms, deconvolution for the instrument response, simulation of the WA seismometer (sensitivity: 2800) and high-pass filtering ($f > 1$ Hz). Being R the hypocentral distance in km, M_L is calculated following the Hutton & Boor formula: (Hutton & Boore, 1987)

$$M_L = \log_{10} A + 1.110 \log_{10}(R/100) + 0.00189(R - 100) + 3 \quad (3)$$

For a meaningful and robust comparison between TM detections and the templates catalogs, the magnitude of the latter have been also calculated using the same approach above.

3 Results and Discussion

3.1 Quality of the hypocenter location

The template-matching catalog consists of $\sim 20,000$ new events, a 5-fold increase with respect to the starting 3992 templates. Since an enriched, high-resolution catalog can be used for the characterization of spatio-temporal pattern of seismicity and/or for an improved imaging of fault systems, it is crucial to provide high-quality hypocenter solutions that, in terms of uncertainty, are comparable to the data already available. Therefore, to evaluate the goodness of the TM detections we compare the quality parameters of the hypocenter solution with those of the templates (Fig. 3). Regarding the error on the horizontal component, the template-matching catalog shows a slightly skewed distribution with a median value of 0.98 km, as opposed to the well peaked distribution for the templates with 0.59 km as median value. The two catalogs differ the most when the vertical error is considered. The two medians show a difference of ~ 0.77 km (1.19 vs. 1.96 km, for the templates and detections, respectively) with a distribution for the detections being again rather skewed. Such discrepancy can be advocated to the substantially different amount of phases (and thus stations) used for obtaining the hypocenter solution for the two different datasets. As shown in Fig. 3, templates' hypocenters are constrained on average with 80% more arrivals (10 vs. 18) with respect to the detections. Consequently, the template-matching detections also suffer from a slightly higher azimuthal gap (126° vs 100°). Overall, considered the significant amount of picks available for the template events and their better azimuthal coverage, it is remarkable that the events obtained by template-matching show only a slightly higher uncertainty of the hypocenter solution. Such homogeneity of the quality of the two datasets is a solid basis for their combined use in any further analysis for which well constrained hypocenters are a prerequisite.

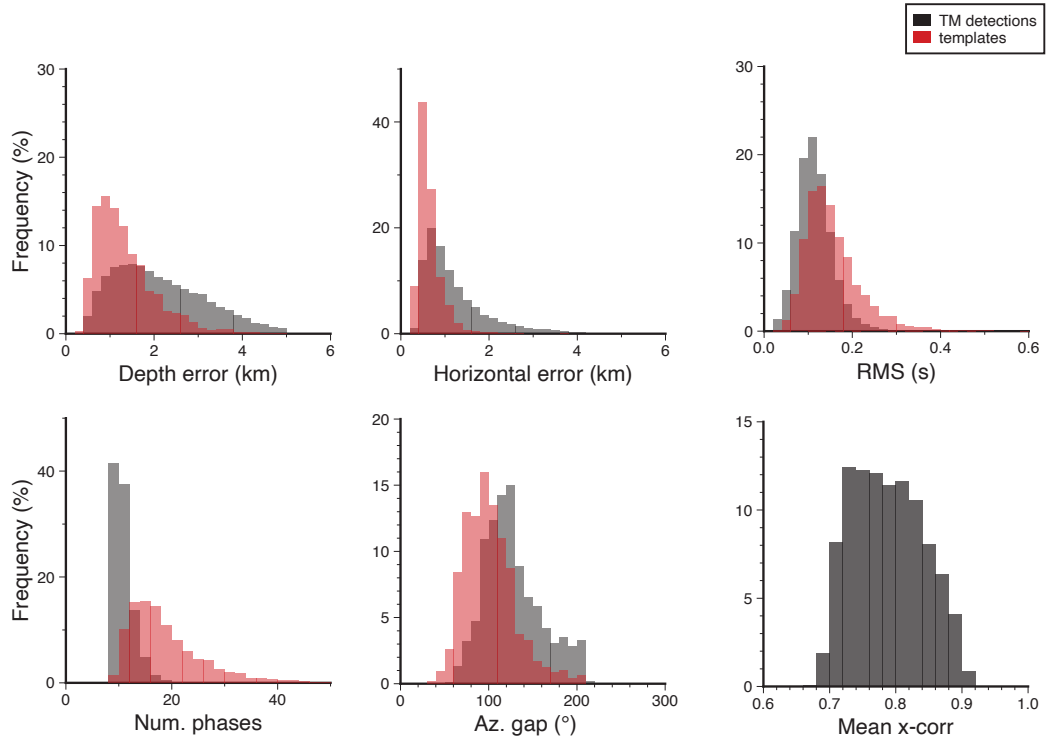


Figure 3. Quality parameters of the hypocenter solutions for the template-matching catalog (gray) and the templates catalog (red). In the lower right corner, the histogram of mean cross-correlation of TM detection with their templates.

3.2 Templates vs. TM-detections

The map in Fig. 4 (left) shows the earthquake locations determined using the same 1-D velocity model (see section 2.3) for both the templates (red) and detected events (black). Though the large overlapping of events, it remains evident that template-matching allowed the recovery of a considerable amount of previously missing seismicity. As expected from a method based on measures of waveforms' similarity, such new seismicity falls in the close vicinity of the templates (less than 5 km for 97% of the detections). This is consistent with previous works showing the decay of waveform coherence for increasing distances between templates and detections. As an example, a synthetic sensitivity study in Schaff (2010) shows that detections with a $x\text{-corr} > 0.7$ (83% of detected events in our case) can be found up to 10-13 km from their template. In a real case scenario, such distance is reduced due to subsurface heterogeneities, differences in event magnitude, fault rupture, focal mechanism and duration.

Templates and detections show the same overall distribution at depth (see panel b in Fig. 5) and in both cases most of the seismicity is confined within 10 km depth. Panel a) in Fig. 5 shows the mean depth of seismicity of the newly detected events in the entire study region, in a 2x2 km bin. The map highlights the shallow to very-shallow seismicity (depth ~ 5 km) of the large and long-lasting Mt. Pollino sequence, that contribute to the pronounced peak of the depth distribution shown in panel b) at around 5 km depth. Overall, the depth of the seismicity does not seem to follow a particular spatial pattern, except for northern part of the study area. Here, in fact, abundant seismicity is found along the axis of the Southern Apennines chain, as well as in its external part towards the foreland domain. Interestingly, earthquake locations are found at increasing depths moving eastwards, thus suggesting a deeper brittle-to-ductile transition and potentially thicker seismogenic zone. Chiarabba and De Gori (2016) suggested that the variable distribution of hypocentral depths along the Apennines can be correlated with areal changes in heat-flow, an explanation that would likely holds for this area as well. The recovery of deep and previously missed seismicity in the external domain of the Southern Apennines can have a direct implication in the evaluation of the seismic hazard of the area, due to relevant potential for a large magnitude usually associated with large seismogenic thickness (see section 3.3).

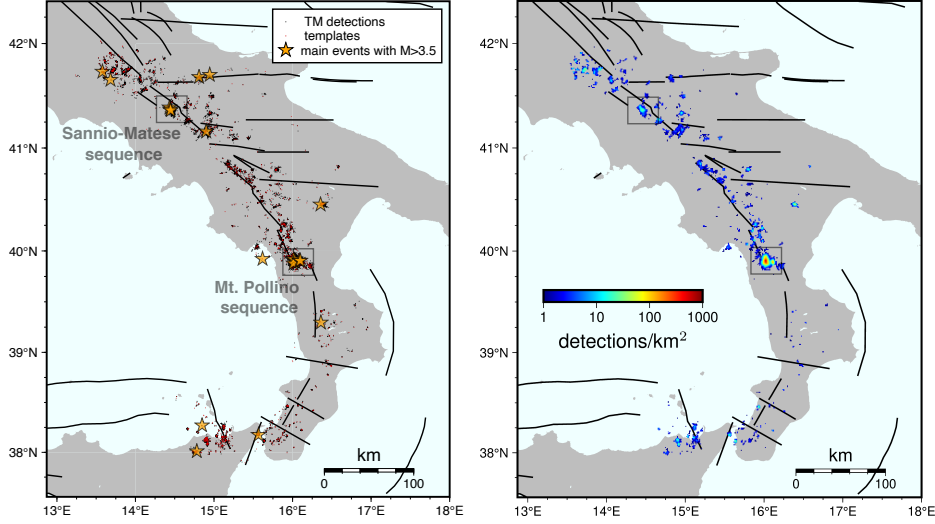


Figure 4. Left: map of the events used as templates (red) superimposed to new events obtained through template-matching. The orange stars represent the $M_L > 3.5$ events occurred between 2009 and 2014 while the black boxes highlights the location of the two main seismic sequences in the same time period. Right: density plot of the detection as number of events in a 1×1 km bin. Black lines indicates major seismogenic faults ($M > 5.5$) as in the DISS database (<https://doi.org/10.13127/diss3.3.0>)

In the right panel of Fig. 6 we plot the mean cross-correlation between each detected event and its template against the two other (main) predictor for waveform similarity: the difference in magnitude and the inter-event horizontal distance. The right panel clearly shows that within 5 km distance, both highly similar (cross-correlation > 0.9) as well as dissimilar (cross-correlation < 0.7) events are found. However, regardless the distance, almost the totality of high-correlation events are found within 10^7 s (~ 4 months), which appears to be a rather sharp threshold beyond which waveform coherence starts to heavily degrade.

In Fig. 6 (left side) we show the same plot as before except for another predictor of waveform similarity, being the magnitude difference between each detection and its template. As expected, events with the highest correlation show similar magnitude to their template, with waveform sharply degrading when magnitude difference increases. The plot shows two, well separate clusters: i) the first refers to detections usually within two unit of magnitude from their templates, occurring within minutes or few days from their template (e.g. 10^6 s ≈ 11 days) and showing a medium to high value of cross-correlation;

ii) the latter (in the order of 10^3 events, be aware of the distortion effect of the logarithmic scale) consists of events significantly smaller ($\Delta M_L < -3$), highly dissimilar to their template, and up to three years apart from these. Regarding this particular cluster, it is worth noting that the low cross-correlation and large difference in magnitude of its events might rise the concern that such events might be false positives, a possibility that is problematic to discern for such low-magnitude events close or below noise level. However, the observation of a rather sharp boundary at a inter-event distance of $\sim 10^7$ s (beyond which the detection of highly similar event become unlikely) can be mainly explained as result of temporal clustering of seismicity.

In addition, we speculate that also time-varying characteristics of the propagating medium can play a role for the loss of waveform coherence. For example, significant variations in such properties can occur on a small temporal scale (few months) due to cyclical/seasonal processes (e.g. fluid circulation induced by precipitation) and also on larger scale due to tectonic or long-term fluid diffusion processes, or a combination of both. For example, time-lapse tomography spanning several years in the Irpinia region (De Landro et al., 2022) has highlighted substantial variation in the V_P , V_S and V_P/V_S velocity structure, in the upper as well as in the middle crust. Multi-annual variation of the ground water level in the shallow karst aquifers have been invoked to explain such changes in the velocity structure, as well as in the crustal deformation and seismicity rate (D’Agostino et al., 2018).

In Fig. 7 (top) we show the cumulative number of events vs. time, for detected events and the templates. The two curves depart from each other as early as in the beginning of 2009, with a sharp increase of the seismicity rate during 2011 in the template-matching catalog, apparently unrelated to any major seismic event. From the second half of 2012, we observe the highest increase in the number of events due the highly productive, swarm-like Mt. Pollino sequence that peaked with two M5 events (Totaro et al., 2013, 2015; Passarelli et al., 2015; Cheloni et al., 2017). Such increase is visible in the template catalog but even more prominent in the detection catalog. From beginning 2013, while the seismicity rate appears to drop towards the background value, template-matching recovers a large amount of previously missing seismicity at an unprecedented rate with respect to the preceding years. In contrast, such increase in the recorded seismicity is only mild in the template catalog, despite the upgrade of the INGV seismic network (~ 120 vs. ~ 180 active stations from 2009 to 2015). The reason for this likely lies on operational

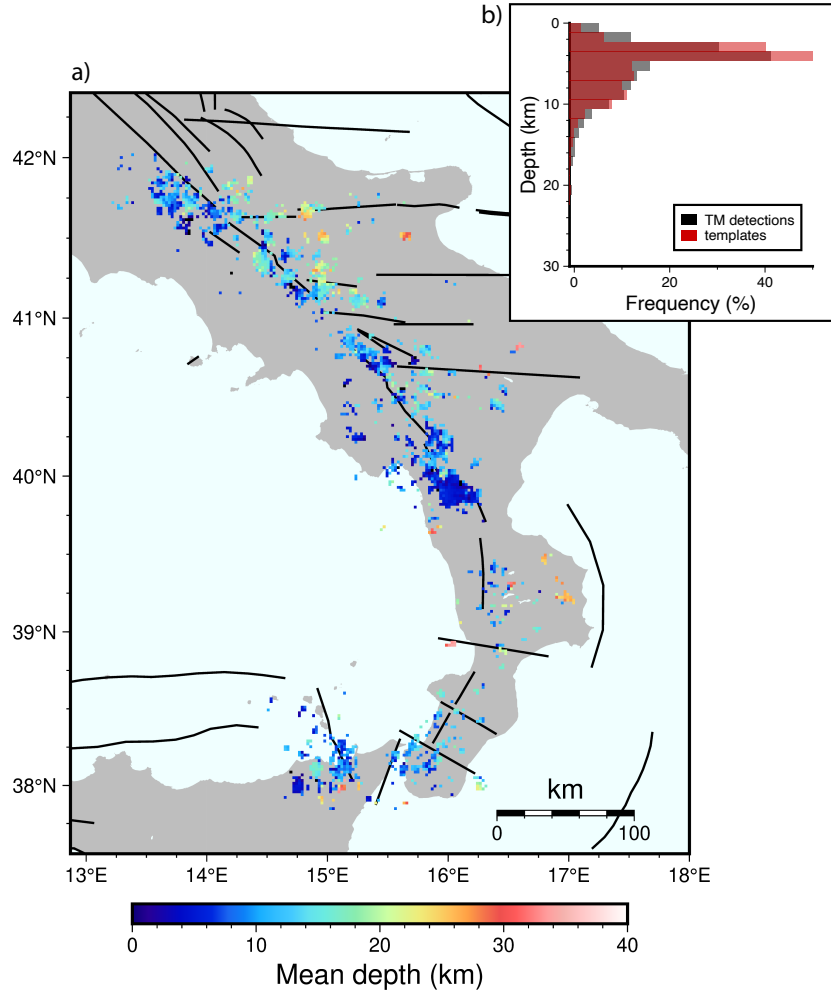


Figure 5. a) Map of mean depth of seismicity (TM-detections and template catalogs) in a block of 2x2 km. Most of events are confined in the 0-15 km range sequence. Note the deepening of the overall seismicity moving eastward with respect to the axis of the Southern Apennines chain. Black lines indicates major seismogenic faults ($M > 5.5$) as in the DISS database (<https://doi.org/10.13127/diss3.3.0>). b) Distribution of the hypocentral depth for the TM-detections and templates.

criteria that are currently used for the construction of the official BSI catalog (only events with $M > 1.5$ are routinely revised by operators), hampering the location of the small magnitude seismicity (Di Maro et al., 2022). This work demonstrate that an *a-posteriori* analysis of data through template-matching, if accompanied to the classical STA/LTA methods commonly used for real-time detection, can lead to a dramatic improvement in the recovery of seismicity. The bottom panel in 7 shows the time series of templates

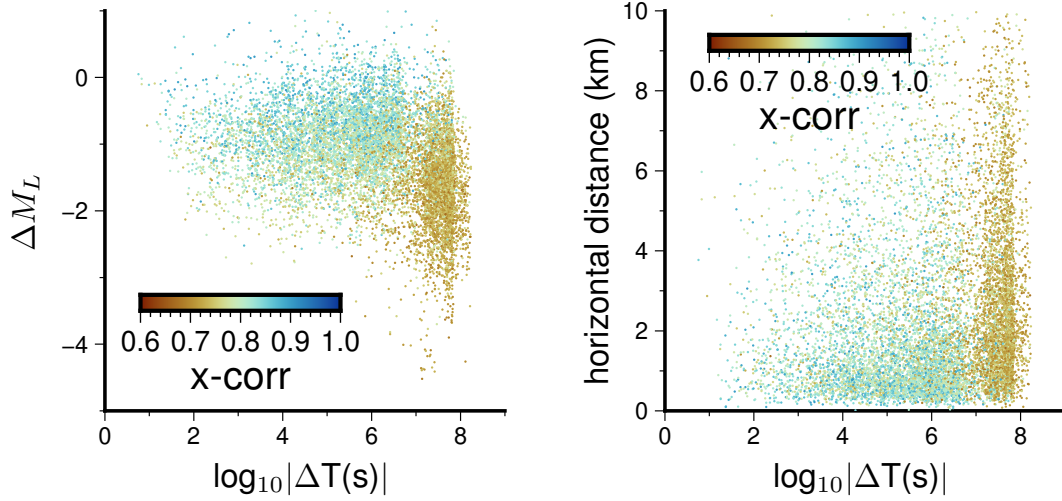


Figure 6. Left: Temporal inter-event distance between detections and templates vs. their magnitude difference. Right: Temporal inter-event distance between detections and templates vs. their horizontal distance. Datapoints in both plots are color-coded according to the cross-correlation value of each detected event.

Table 2. Estimates of magnitude of completeness using three different methods (ZMAP software, Wiemer (2001))

	Max-curvature	BestCombo	MC90
template	1.6	1.9	1.6
template + TM-detections	0.6	1.6	0.3

(red) and detected events by TM. Most of the newly detected seismicity is confined in the 0 to 1 magnitude range. Particularly for the post-2012 period (after the Mt. Pollino sequence) where the seismicity rate is rather uniform, the newly detected events appear to form a background, low-magnitude seismicity apparently unrelated to the $M > 3$ main events occurring in the same period. Finally, to quantify the enrichment of starting template catalog when adding the TM-detections, we estimated the magnitude of completeness using three different methods (Max Curvature, BestCombo and MC90, Wiemer (2001)). As shown in 2 and Fig. 8 each method shows a decrease in magnitude of completeness ranging from 1.3 magnitude unit with MC90 to 0.3 magnitude unit if BestCombo is employed.

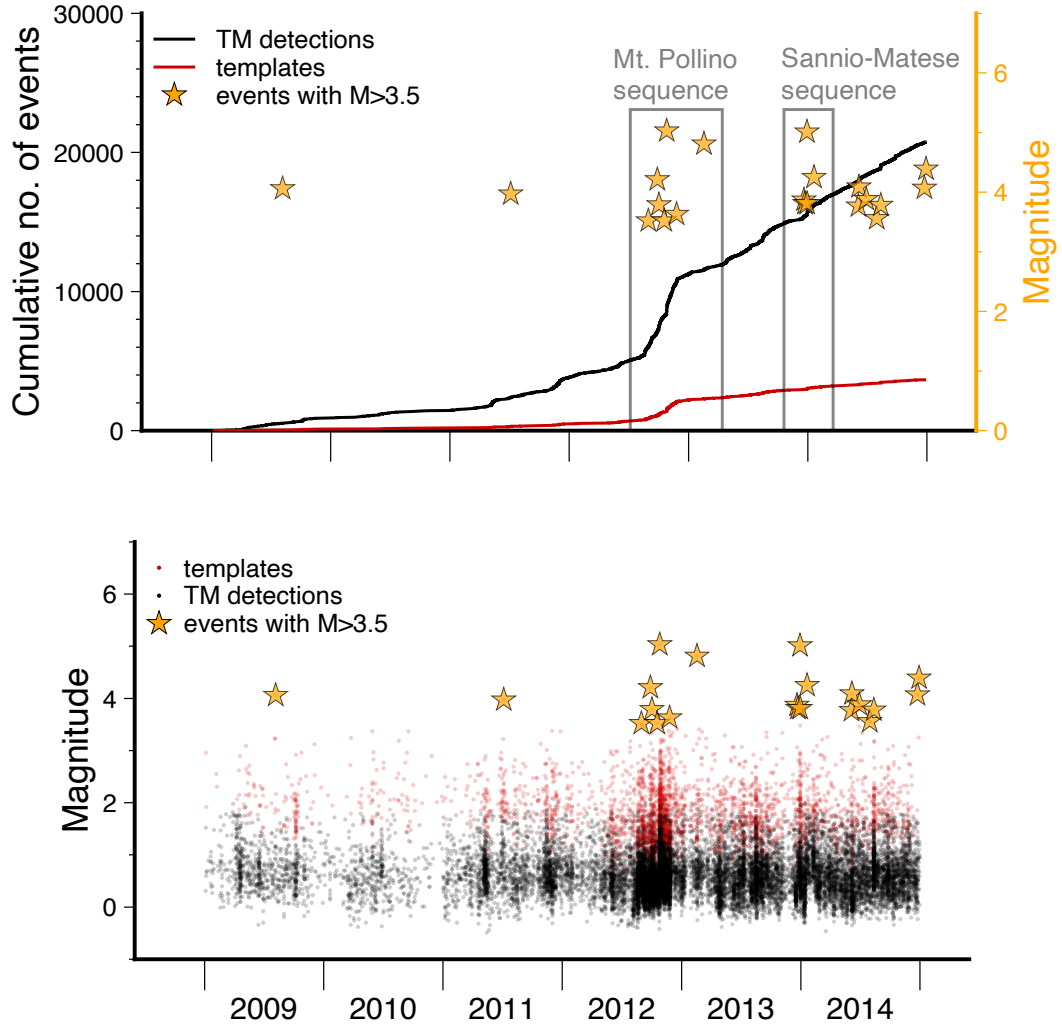


Figure 7. Top: cumulative curves of template events (red) and template-matching detection (black). Orange stars indicate the event with $M > 3.5$ occurring in the study area between 2009 and 2014. Bottom: Distribution of magnitude vs. time of events for templates and TM-detection. As the above panel, main events are superimposed.

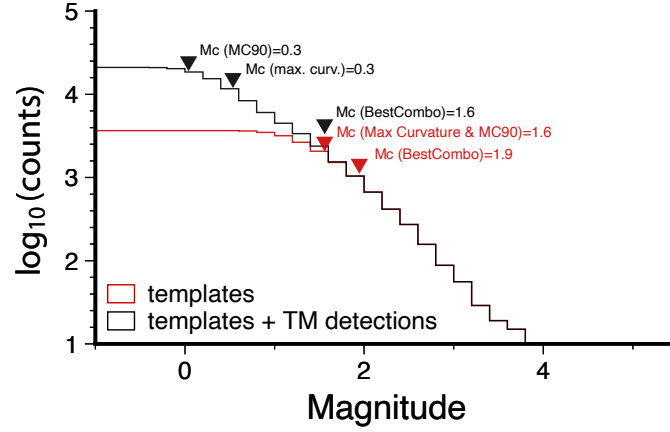


Figure 8. Cumulative frequency-magnitude distribution for the templates (red) and the enriched catalog (black) obtained by adding the events detected by template-matching.

In the following sections, we focus on the Sannio-Matese area and the hidden seismicity recovered through template-matching. In particular, we show the contribution of our enhanced catalog in the characterization of the local seismicity, in light of the known seismotectonic context. For sake of completeness, in both cases we integrated the templates' and detections' catalogs with all the events from the Italian Seismic Bulletin (BSI), whose hypocentral location have been determined using the method and the velocity model described in Section 2.3. Then, all events have been relocated with double-difference technique (Waldhauser & Ellsworth, 2000) in order to improve the imaging of possible fault structure through the well-constrained hypocenter locations.

3.3 The Sannio-Matese area

The Sannio-Matese area is located at the transition between the central and southern part of the Apennines chain, the east verging fault-and-thrust belt accreted since Miocene due to the subduction of Adriatic plate (Faccenna et al., 2001; Gattacceca & Speranza, 2002; Faccenna et al., 2014). Since the Quaternary, the Apennines belt has experienced a NE-SW directed extension, mainly accommodated by NW-SE striking, newly formed normal faults, or by reactivated and inverted thrust faults inherited from the past collisional phase. As shown in Fig. 9 (panel A), this extensional belt is characterized by several M6-7 historical earthquakes, thus posing a substantial seismic hazard (Rovida et al., 2020). According to geological and paleoseismic surveys, the main seismogenic sources are NW-trending normal fault systems bounding the southwestern and northeastern sides

353 of the Matese massif (Boncio et al., 2022): the Aquae Iuliae fault to the west, causative
354 source of the 1349 M6.7 earthquake (P. A. C. Galli & Naso, 2009) and the Bojano fault
355 system to the east, source of the 1805 M 6.6 earthquake (P. Galli et al., 2017; Ferrarini
356 et al., 2017). Moving to SE, a M7 earthquake struck Benevento in 1688, the main mu-
357 nicipality in the Sannio region (Fig. 9, panel A). In the database of Italian seismogenic
358 sources, the 1688 destructive earthquake is associated to a NW-SW striking and NE dip-
359 ping extensional structure, but large uncertainties still remain regarding the geometry
360 of the causative fault (DISS, 2021), as well as of the sources of the M6+ earthquakes that
361 hit the southern Sannio in 1702, 1732 and 1962 (Fig. 9, panel A).

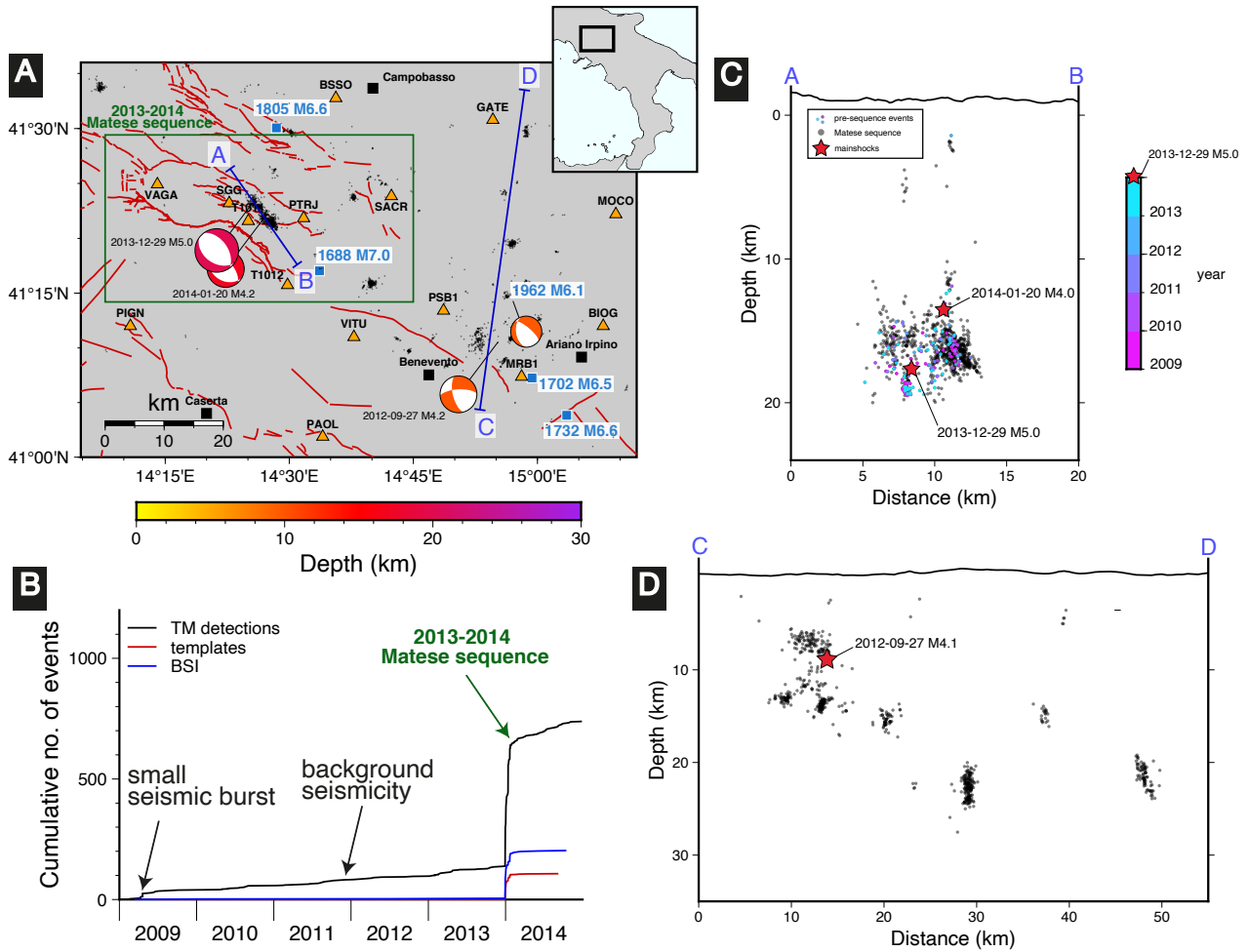


Figure 9. **A):** Map of the Sannio-Matiese area. Beachballs indicate the focal mechanism of the three main events occurred in the area between 2009 and 2014. The 2013-2014 Matiese sequence is highlighted with a green box. Superficial traces of capable faults are in red (ITHACA Working Group, 2019). Blue squares indicate the proposed epicenters for large historical earthquakes (e.g. 1805 and 1688). The focal mechanism of the 1962 M6.1 earthquake is from Westaway (1987). As black dots, the double-difference relocated events detected in this study through template-matching, in addition to their template and other events in the Bollettino Sismico Italiano (BSI). **B):** cumulative number of events in the area of the Matiese sequence. The events recovered through template-matching (black) reconstruct the background seismicity of the area, otherwise seismically silent as far as the officially catalogued events are concerned (in red and blue the curves for the template events and those in the BSI, respectively). A small seismic burst was detected in the first half of 2009. **C):** depth profile along the AB trace cutting the 2013-2014 Matiese sequence (in black). The pre-sequence events are color-coded according to the year of occurrence. The red stars represent the mainshocks of the sequence. **D):** depth profile along the CD trace in the Sannio area, showing the events recovered through template-matching. Note the deepening of the overall seismicity.

3.3.1 The 2013-2014 Matese seismic sequence

On December 29th 2013 a $M_W 5$ event occurred beneath the Matese massif at 17 km depth (Fig. 9, panel A). It was followed by an aftershock sequence that rapidly migrated towards SE. About 22 days later a $M_W 4.2$ earthquake struck in the vicinity of the mainshock (De Gori et al., 2014). In both cases the fault plane solution suggested a rupture along a NW-striking, steep normal fault that likely dips SW-wards (Ferranti et al., 2015). Afterwards, the overall seismicity decayed and completely ceased by February 2014. While the past background seismicity and weak sequences ($M < 3$) recorded in the Sannio-Matese are confined in the upper crust (e.g. Bisio et al. (2004), among others) the 2013-2014 sequence was unusually deep (15-20 km depth-). Given the peculiar finger-like distribution of the seismicity and the type and pattern of amplitude attenuation, this sequence has been related to fluid over-pressure and migration of deep melts rather than tectonic stress release (Di Luccio et al., 2018). The upward migrating aftershocks defined two separate clusters, laterally separated by a 1.5 km-wide, dike-like aseismic volume that was interpreted as indicative of a stagnating intrusive body (Di Luccio et al., 2018). Strictly considering the area of the 2013-2014 sequence (green box in Fig. 9, panel A), the events catalogued in the BSI and then relocated at the double difference amount to 312 (108 of which have been used as templates in this study). Interestingly, the area appeared seismically silent in the years preceding the 2013-2014 sequence. However, by applying the template-matching technique we obtained a substantial enrichment of the seismic catalog during the 2013-2014 sequence, as well as in previous years. As shown in the cumulative plot of events in Fig. 9 (panel B), from 2009 until the $M 5$ mainshock of December 2013, TM allowed us to detect +100 events, as opposed to only four, good quality events, cataloged by INGV in the same time period. Interestingly, less than half of the newly detected events belongs to a small seismic burst in the first half of 2009 (see Fig. 9, panel B), for which no record exists in the official catalog. The templates that led to such new detections belong to the 2013-2014 sequence, implying an inter-event temporal distance of the template-detection pairs of about 4.5 years. Interestingly, despite the large temporal distance, the detected events show a cross-correlation around 0.8, implying a rather high degree of resemblance. This represent a remarkable observation, in light of the generalized dissimilarity between template and detections that accrue in only few months in the rest of the catalog, as shown and discussed in Section 3.2.

After the minor seismic burst in 2009, template-matching has revealed a rather constant-rate seismicity (Fig. 9 panel B) which represents, a previously unnoticed, small-magnitude background activity. The AB profile (Fig. 9, panel C) shows the distribution in depth of the 2013-2014 Matese sequence (in black) as opposed to the pre-sequence events obtained through TM, occurring as early as in 2009. Overall, these events spread across the entire zone where the Matese sequence later occurred, with a noticeable clustering of earlier events (i.e. 2009) in the SE sector and just below the hypocenter of the 2013 mainshock. The pre-sequence events occurring in 2013 are spread in the entire area as well, but also tend to concentrate in the vicinity of the mainshock. However, the analysis of the space-time distribution of this pre-sequence seismicity does not show any peculiar migration pattern. Strictly considering the sequence period, templates-matching allowed to double the number of aftershocks in comparison to the originally catalogued events. While these show a sharp decline in the seismicity rate, implying a ceasing seismic activity in the second half of 2014, template-matching has recovered more than 100 events in the same period. Only at the end of 2014 the number of detected events appear to reach a plateau that approaches the level of pre-sequence seismic activity.

Owing to the absence of recorded seismicity before the Matese sequence (see the red and blue cumulative curves in Fig. 9, panel B), in their work Di Luccio et al. (2018) excluded the hypothesis of a steady accumulation of magma, upholding the scenario of sudden and episodic dike intrusion and subsequent seismic burst. In light of our results that have unravelled a constant, small-magnitude, background seismicity in the mainshock zone preceding the Matese sequence, we suggest a scenario that is typical of volcanic environment (McNutt & Roman, 2015; Traversa & Grasso, 2010). It generally consists of alternating distribution of volcano-tectonic earthquakes between episodic burst, with a constant-rate seismicity during the inter-eruptive phases. In this regard, it is instructive to compare the black curve in panel B in Fig. 9 with the long recording of cumulative volcano-tectonic events of the Mt. Etna in Traversa and Grasso (2010), showing a clear pattern of steady background activity and sudden surges in seismicity, corresponding to dike emplacement and subsequent eruptions.

In conclusion, our new data can stimulate a better understanding of such peculiar seismic sequence. As an example, we suggest that the cluster of pre-sequence microseismicity located near the mainshock nucleation could provide evidence for the presence of a preparatory phase. Moreover, the retrieval of the pre-sequence, background seismic-

ity might clarify the possible role of fluid circulation and/or other hydrological contributors in modulating the magnitude and spatio-temporal characteristics of seismicity in the Matese area, similarly to what observed for other seismogenic zones in the Apennines (D’Agostino et al., 2018).

3.3.2 *Seismicity distribution in the Sannio area*

The southern Apennines features two different seismotectonic domains: the narrow extensional belt along the range axis and a deep shear zones under the external Apennines towards the foreland in the east (Fracassi & Valensise, 2007; Pino et al., 2008; Di Luccio, Fukuyama, & Pino, 2005; Di Luccio, Piscini, et al., 2005; Ciaccio et al., 2021). In the former domain, moderate to large earthquakes show extensional mechanisms striking NW-SE (1980 M6.9 Irpinia earthquake, 1998 M5.6 Castelluccio, 2013-2014 M5.0 Matese sequence, 2011-2014 Pollino sequence) and the seismogenic layer is about 10-15 km thick (Chiarabba et al., 2005; Latorre et al., 2022). With the only exception of the Matese seismic sequence described in the previous section, this observation is clearly evidenced in Fig. 5 which displays a clear concentration of events at depth around 5 km, followed by a sharp decline below 10 km. In contrast, the the external Apennines domain has been characterized by moderate strike-slip earthquakes (1990 M5.7 Potenza, 2002 M5.9 Molise) along E-W structures at mid- to lower-crustal depths within the Apulian plate. However, such a regional seismotectonic zonation seems inappropriate for the region encompassing the southern Sannio and northern Irpinia, that was struck by M6+ earthquakes in 1702, 1732, 1962 (see Fig. 9, panel A). For the 1962 sequence, published focal solutions for the two M~6 shocks are debated and vary from NW-striking transtensional mechanism Westaway (1987) to E-W striking pure strike-slip mechanism Vannoli et al. (2016), although their hypocenters have been located at upper crustal depths (< 10 km). In September 2012, a $M_W 4.2$ earthquake occurred in this region at a depth of ~10 km (<http://inside.rm.ingv.it/event/1335371>) and published focal solutions varies again from a NW-trending transtensional mechanism Scognamiglio et al. (2006) to a pure strike-slip mechanism trending E-W (Adinolfi et al., 2015). Extensional to strike-slip rupture mechanisms also characterize the local background seismicity recorded in 2014-2016 (De Matteo et al., 2018). Based on these observations, the Sannio-Irpinia boundary has been regarded as a complex transitional zone where the seismotectonic setting changes both in the SW-NE direction as well as in depth (Adinolfi et al., 2015; De Matteo et al., 2018),

with an extensional regime confined in the first 15 km, superimposed to a transcurrent
 one at mid-lower crustal depth that characterizes the external part of the belt. Our new
 template-matching catalog provides valuable information on the complex seismotectonic
 setting of this region. The CD profile in Fig. 4 (panel D) that runs SSW-NNE from the
 axial to the external portion of the Apennines reveals a clear NE-wards deepening of seis-
 micity. In the southernmost part of the profile (about 10 km NE of the city of Benevento),
 seismicity is confined in the upper crust (< 15 km depth) and appears to concentrate
 in two distinct depth levels, 5-9 km and 11-15 km. In the outer belt, two remarkable ver-
 tical clusters are found at substantially greater depth (20-25 km), consistent with the
 overall deepening of seismicity shown in Fig. 5, when moving towards the external Apen-
 nines. The template-matching catalog displays, for the first time, that the eastward deep-
 ening of the seismicity is extremely rapid: the cut-off of the background seismicity in-
 creases from 15 to 25 km depth in about 10-12 km distance (Fig. 9, panel D), consid-
 ering that the profile D is not exactly perpendicular to the belt axis. If we take into ac-
 count our re-location of the 2012 $M_W 4.2$ earthquake, this is coherent with the the west-
 ern seismicity confined in the upper crust. For both the mid-crustal clusters, seismic-
 ity persisted during the whole 2009-2014 interval, illuminating two vertical structures
 covering more than 5 km in depth. A comparison with the catalog of the 2014-2016 seis-
 micity ($M < 3$) of De Matteo et al. (2018) and obtained through standard detection tech-
 niques unravels that these two vertical clusters were also active in the following years.
 Moreover, the focal mechanisms of the best located events of De Matteo et al. (2018) in
 the two deep vertical clusters show a clear E-W trending, strike-slip dextral mechanisms,
 whereas the seismicity located NE of Benevento and confined in the upper crust have
 NW-SE trending extensional kinematics (see Figure 4 in De Matteo et al. (2018)). In
 conclusion, previous works and our new results, taken collectively, indicate that an abrupt
 deepening and change in the tectonic style, from normal to strike-slip, occurs in the NE-
 direction at the border between the southern Sannio and the northern Irpinia region. Co-
 herently, the comparison of our template-matching catalog with the stress field inver-
 sion of De Matteo et al. (2018) favors an extensional rupture mechanism for the debated
 1962 M_6 and 2012 $M_w 4.2$ earthquakes. The emergence of two vertical, km-scale struc-
 tures with strike-slip dextral kinematics, at mid-crustal depth in the Apulian plate has
 a significant implication for seismic hazard. Such structures may represent silent seis-
 mogenic fault that are analogue to the dextral E-W shear-zones that ruptured SE-wards

and NE-wards of the Sannio-Irpinia region during the 1990, such as the 1990 M5.7 Potenza and the 2002 M5.9 Molise deep sequences.

4 Conclusion

We have produced the first high-resolution seismic catalog at regional scale for the Southern Apennines (Italy), employing a template-matching (TM) technique. We used 4.000 templates that allowed us to detect about 20.000 new seismic events. Located with the same smooth, average 1D velocity model, the templates and the newly detected events show comparable quality of the hypocenter solution. The events retrieved by template matching have magnitudes confined in the 0-1 range, reaching values as low as -0.5, thus leading to an improvement of the magnitude of completeness that, depending on the method employed, shows a decrease of about one unit.

To show the potential of the template-matching catalog for the understanding of the spatio-temporal seismicity distribution and its possible impact for the assessment of the seismic hazard, we focus on the Sannio-Matese area.

i) Regarding the 2013-2014 Matese sequence, TM successfully recovered a substantial amount of previously undetected seismic activity, revealing a sudden surge of seismicity more than three years before the Matese sequence. Additionally, we retrieved the small-magnitude, constant-rate, background seismicity occurring in the immediate vicinity of the M5 mainshock and subsequent 2013-2014 sequence. Such background activity was not reported in the starting catalogs. In fact, this area was considered seismically silent for the time preceding the 2013-2014 sequence.

ii) Located at the border of the Southern Apennines belt axis towards the outer belt, the Sannio area shows a rapid deepening of the seismic activity unravelled by template matching. In fact, moving from SSW to NNE (from the internal to the external portion of the Apennines belt), hypocenters concentrate between 20 and 25 km, rather than 5-10 km. Such observation, combined with evidences on the focal mechanism of past events, suggest that the Sannio area can be regarded as a complex area characterized by a sharp thickening of the seismogenic layer and change of the deformation style, from pure extensional to transtensive/strike-slip.

5 Data Availability Statement

The raw seismic recordings are available from the network repositories: IV (INGV Seismological Data Centre, 1997) (<https://webservices.ingv.it/fdsnws/dataselect/1/>), MN (MedNet Project Partner Institutions, 1988 (<https://webservices.ingv.it/fdsnws/dataselect/1/>)), IX (Irpina Seismic Network) (<https://webservices.ingv.it/fdsnws/dataselect/1/>). The code Eqcorrscan (Chamberlain et al., 2018) was used for running the template-matching algorithm. The code NonLinLoc (Lomax et al., 2000) was used for determining the earthquake locations. All figures were made using PyGMT(Uieda et al., 2023).

Acknowledgments

G. Diaferia acknowledges funding provided by the Italian Minister of Research in the framework of the PRIN-2017 project MUSE 4D (2017KT2MKE) Overtime tectonic, dynamic and rheologic control on destructive multiple seismic events—Special Italian Faults and Earthquakes: From real 4-D cases to models. G. Diaferia was also supported by the FURTHER project “The role of FIUIDs in the pReparaTory pHase of EaRthquakes in Southern Apennines” funded by the Strategic Earthquake Department of Istituto Nazionale di Geofisica e Vulcanologia (Italy). The authors thank Daniele Melini for his valuable support with the HPC infrastructure at INGV.

References

- Adinolfi, G. M., De Matteis, R., Orefice, A., Festa, G., Zollo, A., de Nardis, R., & Lavecchia, G. (2015). The september 27, 2012, ml 4.1, benevento earthquake: A case of strike-slip faulting in southern apennines (italy). *Tectonophysics*, 660, 35–46.
- Allen, R. (1982). Automatic phase pickers: Their present use and future prospects. *Bulletin of the Seismological Society of America*, 72(6B), S225–S242.
- Beaucé, E., Frank, W. B., & Romanenko, A. (2018). Fast matched filter (fmf): An efficient seismic matched-filter search for both cpu and gpu architectures. *Seismological Research Letters*, 89(1), 165–172.
- Bisio, L., Di Giovambattista, R., Milano, G., & Chiarabba, C. (2004). Three-dimensional earthquake locations and upper crustal structure of the sannio-matese region (southern italy). *Tectonophysics*, 385(1-4), 121–136.
- Boncio, P., Auciello, E., Amato, V., Aucelli, P., Petrosino, P., Tangari, A. C., &

- 553 Jicha, B. R. (2022). Late quaternary faulting in the southern matese (italy):
554 implications for earthquake potential and slip rate variability in the southern
555 apennines. *Solid Earth*, 13(3), 553–582.
- 556 Chamberlain, C. J., Boese, C. M., & Townend, J. (2017). Cross-correlation-based
557 detection and characterisation of microseismicity adjacent to the locked, late-
558 interseismic alpine fault, south westland, new zealand. *Earth and Planetary
559 Science Letters*, 457, 63–72.
- 560 Chamberlain, C. J., Hopp, C. J., Boese, C. M., Warren-Smith, E., Chambers, D.,
561 Chu, S. X., ... Townend, J. (2018). Eqcorrscan: Repeating and near-repeating
562 earthquake detection and analysis in python. *Seismological Research Letters*,
563 89(1), 173–181.
- 564 Chamberlain, C. J., Shelly, D. R., Townend, J., & Stern, T. A. (2014). Low-
565 frequency earthquakes reveal punctuated slow slip on the deep extent of the
566 alpine fault, new zealand. *Geochemistry, Geophysics, Geosystems*, 15(7),
567 2984–2999.
- 568 Cheloni, D., D’Agostino, N., Selvaggi, G., Avallone, A., Fornaro, G., Giuliani, R., ...
569 Tizzani, P. (2017). Aseismic transient during the 2010–2014 seismic swarm:
570 evidence for longer recurrence of m 6.5 earthquakes in the pollino gap (south-
571 ern italy)? *Scientific reports*, 7(1), 1–10.
- 572 Chiarabba, C., & De Gori, P. (2016). The seismogenic thickness in italy: constraints
573 on potential magnitude and seismic hazard. *Terra Nova*, 28(6), 402–408.
- 574 Chiarabba, C., Jovane, L., & DiStefano, R. (2005). A new view of italian seismicity
575 using 20 years of instrumental recordings. *Tectonophysics*, 395(3-4), 251–268.
- 576 Ciaccio, M. G., Di Stefano, R., Improta, L., Mariucci, M. T., & Group, B. W.
577 (2021). First-motion focal mechanism solutions for 2015–2019 m 4.0 italian
578 earthquakes. *Frontiers in Earth Science*, 9, 630116.
- 579 D’Agostino, N., Silverii, F., Amoroso, O., Convertito, V., Fiorillo, F., Ventafridda,
580 G., & Zollo, A. (2018). Crustal deformation and seismicity modulated by
581 groundwater recharge of karst aquifers. *Geophysical Research Letters*, 45(22),
582 12–253.
- 583 De Barros, L., Cappa, F., Deschamps, A., & Dublanchet, P. (2020). Imbricated
584 aseismic slip and fluid diffusion drive a seismic swarm in the corinth gulf,
585 greece. *Geophysical Research Letters*, 47(9), e2020GL087142.

- 586 De Gori, P., Moretti, M., Margheriti, L., Cecere, G., Govoni, A., Criscuoli, F., ...
 587 others (2014). Le attività di pronto intervento sismico dell'ingv a seguito del
 588 terremoto del 29 dicembre 2013 (area del matese). *Rapporti Tecnici INGV*.
- 589 De Landro, G., Amoroso, O., Russo, G., D'Agostino, N., Esposito, R., Emolo, A., &
 590 Zollo, A. (2022). Decade-long monitoring of seismic velocity changes at the
 591 irpinia fault system (southern italy) reveals pore pressure pulsations. *Scientific*
 592 *reports*, 12(1), 1–9.
- 593 De Matteo, A., Massa, B., Milano, G., & D'Auria, L. (2018). A transitional vol-
 594 ume beneath the sannio-irpinia border region (southern apennines): Different
 595 tectonic styles at different depths. *Tectonophysics*, 723, 14–26.
- 596 Di Luccio, F., Chiodini, G., Caliro, S., Cardellini, C., Convertito, V., Pino, N. A., ...
 597 Ventura, G. (2018). Seismic signature of active intrusions in mountain chains.
 598 *Science Advances*, 4(1), e1701825.
- 599 Di Luccio, F., Fukuyama, E., & Pino, N. (2005). The 2002 molise earthquake
 600 sequence: What can we learn about the tectonics of southern italy? *Tectono-*
 601 *physics*, 405(1-4), 141–154.
- 602 Di Luccio, F., Piscini, A., Pino, N., & Ventura, G. (2005). Reactivation of deep
 603 faults beneath southern apennines: evidence from the 1990–1991 potenza seis-
 604 mic sequences. *Terra Nova*, 17(6), 586–590.
- 605 Di Maro, R., Arcoraci, L., Battelli, P., Berardi, M., Castellano, C., Castello, B., ...
 606 others (2022). Bollettino sismico italiano 2015. *Quaderni di Geofisica*.
- 607 DISS. (2021). Database of individual seismogenic sources (diss), version 3.: A
 608 compilation of potential sources for earthquakes larger than m 5.5 in italy and
 609 surrounding area.
- 610 Di Stefano, R., & Ciaccio, M. G. (2014). The lithosphere and asthenosphere system
 611 in italy as inferred from the vp and vs 3d velocity model and moho map. *Jour-*
 612 *nal of Geodynamics*, 82, 16–25.
- 613 Faccenna, C., Becker, T. W., Auer, L., Billi, A., Boschi, L., Brun, J. P., ... others
 614 (2014). Mantle dynamics in the mediterranean. *Reviews of Geophysics*, 52(3),
 615 283–332.
- 616 Faccenna, C., Becker, T. W., Lucente, F. P., Jolivet, L., & Rossetti, F. (2001). His-
 617 tory of subduction and back arc extension in the central mediterranean. *Geo-*
 618 *physical Journal International*, 145(3), 809–820.

- 619 Felzer, K. R., & Brodsky, E. E. (2006). Decay of aftershock density with distance in-
620 dicates triggering by dynamic stress. *Nature*, *441*(7094), 735–738.
- 621 Ferranti, L., Milano, G., Burrato, P., Palano, M., & Cannavò, F. (2015). The seis-
622 mogenic structure of the 2013–2014 matese seismic sequence, southern italy:
623 implication for the geometry of the apennines active extensional belt. *Geophys-*
624 *ical Journal International*, *201*(2), 823–837.
- 625 Ferrarini, F., Boncio, P., de Nardis, R., Pappone, G., Cesarano, M., Aucelli, P. P.,
626 & Lavecchia, G. (2017). Segmentation pattern and structural complexities in
627 seismogenic extensional settings: The north matese fault system (central italy).
628 *Journal of Structural Geology*, *95*, 93–112.
- 629 Fracassi, U., & Valensise, G. (2007). Unveiling the sources of the catastrophic 1456
630 multiple earthquake: Hints to an unexplored tectonic mechanism in southern
631 italy. *Bulletin of the Seismological Society of America*, *97*(3), 725–748.
- 632 Frank, W. B., Shapiro, N. M., Husker, A. L., Kostoglodov, V., Romanenko, A., &
633 Campillo, M. (2014). Using systematically characterized low-frequency earth-
634 quakes as a fault probe in guerrero, mexico. *Journal of Geophysical Research:*
635 *Solid Earth*, *119*(10), 7686–7700.
- 636 Galli, P., Giaccio, B., Messina, P., Peronace, E., Amato, V., Naso, G., . . . others
637 (2017). Middle to late pleistocene activity of the northern matese fault system
638 (southern apennines, italy). *Tectonophysics*, *699*, 61–81.
- 639 Galli, P. A. C., & Naso, J. A. (2009). Unmasking the 1349 earthquake source
640 (southern italy): paleoseismological and archaeoseismological indications from
641 the aquae iuliae fault. *Journal of Structural Geology*, *31*(2), 128–149.
- 642 Gattacceca, J., & Speranza, F. (2002). Paleomagnetism of jurassic to miocene
643 sediments from the apenninic carbonate platform (southern apennines, italy):
644 Evidence for a 60 counterclockwise miocene rotation. *Earth and Planetary*
645 *Science Letters*, *201*(1), 19–34.
- 646 Gibbons, S. J., & Ringdal, F. (2006). The detection of low magnitude seismic events
647 using array-based waveform correlation. *Geophysical Journal International*,
648 *165*(1), 149–166.
- 649 Gutenberg, B., & Richter, C. F. (1944). Frequency of earthquakes in california. *Bul-*
650 *letin of the Seismological society of America*, *34*(4), 185–188.
- 651 Husen, S., & Hardebeck, J. (2011). Understanding seismicity catalogs and their

652 problems. *Community Online Resource for Statistical Seismicity Analysis*.

653 Hutton, L., & Boore, D. M. (1987). The ml scale in southern california. *Bulletin of*
654 *the Seismological Society of America*, 77(6), 2074–2094.

655 Improta, L., Bagh, S., De Gori, P., Valoroso, L., Pastori, M., Piccinini, D., ...
656 Buttinelli, M. (2017). Reservoir structure and wastewater-induced seismic-
657 ity at the val d’agri oilfield (italy) shown by three-dimensional vp and vp/vs
658 local earthquake tomography. *Journal of Geophysical Research: Solid Earth*,
659 122(11), 9050–9082.

660 Improta, L., & Corciulo, M. (2006). Controlled source nonlinear tomography: A
661 powerful tool to constrain tectonic models of the southern apennines orogenic
662 wedge, italy. *Geology*, 34(11), 941–944.

663 Improta, L., De Gori, P., & Chiarabba, C. (2014). New insights into crustal struc-
664 ture, cenozoic magmatism, co2 degassing, and seismogenesis in the southern
665 apennines and irpinia region from local earthquake tomography. *Journal of*
666 *Geophysical Research: Solid Earth*, 119(11), 8283–8311.

667 ITHACA Working Group, I. H. f. C. f. (2019). A database of active capable faults
668 of the italian territory. available online: [http://sgi2.isprambiente.it/](http://sgi2.isprambiente.it/ithacaweb/Mappatura.aspx)
669 [ithacaweb/Mappatura.aspx](http://sgi2.isprambiente.it/ithacaweb/Mappatura.aspx). *ISPRA Geological Survey of Italy*.

670 Kato, A., Obara, K., Igarashi, T., Tsuruoka, H., Nakagawa, S., & Hirata, N. (2012).
671 Propagation of slow slip leading up to the 2011 m w 9.0 tohoku-oki earth-
672 quake. *Science*, 335(6069), 705–708.

673 Kim, W., Hahm, I.-K., Jin Ahn, S., & Hoon Lim, D. (2006). Determining hypocen-
674 tral parameters for local earthquakes in 1-d using a genetic algorithm. *Geo-*
675 *physical Journal International*, 166(2), 590–600.

676 Kissling, E., Ellsworth, W., Eberhart-Phillips, D., & Kradolfer, U. (1994). Initial
677 reference models in local earthquake tomography. *Journal of Geophysical Re-*
678 *search: Solid Earth*, 99(B10), 19635–19646.

679 Latorre, D., Di Stefano, R., Castello, B., Michele, M., & Chiaraluce, L. (2022). An
680 updated view of the italian seismicity from probabilistic location in 3d velocity
681 models: The 1981–2018 italian catalog of absolute earthquake locations (class).
682 *Tectonophysics*, 229664.

683 Lomax, A., Virieux, J., Volant, P., & Berge-Thierry, C. (2000). Probabilistic earth-
684 quake location in 3d and layered models. In *Advances in seismic event location*

- (pp. 101–134). Springer.
- Matrullo, E., De Matteis, R., Satriano, C., Amoroso, O., & Zollo, A. (2013). An improved 1-d seismic velocity model for seismological studies in the campania–lucania region (southern italy). *Geophysical Journal International*, 195(1), 460–473.
- McNutt, S. R., & Roman, D. C. (2015). Volcanic seismicity. In *The encyclopedia of volcanoes* (pp. 1011–1034). Elsevier.
- Mu, D., Lee, E.-J., & Chen, P. (2017). Rapid earthquake detection through gpu-based template matching. *Computers & Geosciences*, 109, 305–314.
- Passarelli, L., Hainzl, S., Cesca, S., Maccaferri, F., Mucciarelli, M., Roessler, D., ... Rivalta, E. (2015). Aseismic transient driving the swarm-like seismic sequence in the pollino range, southern italy. *Geophysical Journal International*, 201(3), 1553–1567.
- Pastori, M., Margheriti, L., De Gori, P., Govoni, A., Lucente, F. P., Moretti, M., ... others (2021). The 2011–2014 pollino seismic swarm: Complex fault systems imaged by 1d refined location and shear wave splitting analysis at the apennines–calabrian arc boundary. *Frontiers in Earth Science*, 9, 90.
- Pino, N., Palombo, B., Ventura, G., Perniola, B., & Ferrari, G. (2008). Waveform modeling of historical seismograms of the 1930 irpinia earthquake provides insight on “blind” faulting in southern apennines (italy). *Journal of Geophysical Research: Solid Earth*, 113(B5).
- Ross, Z. E., Hauksson, E., & Ben-Zion, Y. (2017). Abundant off-fault seismicity and orthogonal structures in the san jacinto fault zone. *Science Advances*, 3(3), e1601946.
- Ross, Z. E., Trugman, D. T., Hauksson, E., & Shearer, P. M. (2019). Searching for hidden earthquakes in southern california. *Science*, 364(6442), 767–771.
- Rovida, A., Locati, M., Camassi, R., Lolli, B., & Gasperini, P. (2020). *The italian earthquake catalogue cpti15. vol. 18*. Springer Netherlands.
- Schaff, D. (2010). Improvements to detection capability by cross-correlating for similar events: a case study of the 1999 xiuyan, china, sequence and synthetic sensitivity tests. *Geophysical Journal International*, 180(2), 829–846.
- Scognamiglio, L., Tinti, E., & Quintiliani, M. (2006). Time domain moment tensor [data set]. *Istituto Nazionale di Geofisica e Vulcanologia (INGV)*, 200610.

- 718 Shearer, P. M. (2002). Parallel fault strands at 9-km depth resolved on the imperial
719 fault, southern california. *Geophysical Research Letters*, 29(14), 19–1.
- 720 Shelly, D. R., Beroza, G. C., & Ide, S. (2007). Non-volcanic tremor and low-
721 frequency earthquake swarms. *Nature*, 446(7133), 305–307.
- 722 Shelly, D. R., Ellsworth, W. L., & Hill, D. P. (2016). Fluid-faulting evolution in
723 high definition: Connecting fault structure and frequency-magnitude variations
724 during the 2014 long valley caldera, california, earthquake swarm. *Journal of*
725 *Geophysical Research: Solid Earth*, 121(3), 1776–1795.
- 726 Shelly, D. R., Hill, D. P., Massin, F., Farrell, J., Smith, R. B., & Taira, T. (2013). A
727 fluid-driven earthquake swarm on the margin of the yellowstone caldera. *Jour-*
728 *nal of Geophysical Research: Solid Earth*, 118(9), 4872–4886.
- 729 Stein, R. S. (1999). The role of stress transfer in earthquake occurrence. *Nature*,
730 402(6762), 605–609.
- 731 Totaro, C., Presti, D., Billi, A., Gervasi, A., Orecchio, B., Guerra, I., & Neri, G.
732 (2013). The ongoing seismic sequence at the pollino mountains, italy. *Seismo-*
733 *logical Research Letters*, 84(6), 955–962.
- 734 Totaro, C., Seeber, L., Waldhauser, F., Steckler, M., Gervasi, A., Guerra, I., ...
735 Presti, D. (2015). An intense earthquake swarm in the southernmost apen-
736 nines: fault architecture from high-resolution hypocenters and focal mecha-
737 nisms. *Bulletin of the Seismological Society of America*, 105(6), 3121–3128.
- 738 Traversa, P., & Grasso, J.-R. (2010). How is volcano seismicity different from tec-
739 tonic seismicity? *Bulletin of the Seismological Society of America*, 100(4),
740 1755–1769.
- 741 Trionfera, B., Frepoli, A., De Luca, G., De Gori, P., & Doglioni, C. (2020). The
742 2013–2018 matese and beneventano seismic sequences (central–southern apen-
743 nines): new constraints on the hypocentral depth determination. *Geosciences*,
744 10(1), 17.
- 745 Uieda, L., Tian, D., Leong, W. J., Schlitzer, W., Grund, M., Jones, M., ... Wessel,
746 P. (2023, March). *PyGMT: A Python interface for the Generic Mapping Tools*.
747 Zenodo. Retrieved from <https://doi.org/10.5281/zenodo.7772533> doi:
748 10.5281/zenodo.7772533
- 749 Valoroso, L., Improta, L., Chiaraluce, L., Di Stefano, R., Ferranti, L., Govoni, A., &
750 Chiarabba, C. (2009). Active faults and induced seismicity in the val d’agri

- 751 area (southern apennines, italy). *Geophysical Journal International*, 178(1),
752 488–502.
- 753 Vannoli, P., Bernardi, F., Palombo, B., Vannucci, G., Console, R., & Ferrari, G.
754 (2016). New constraints shed light on strike-slip faulting beneath the southern
755 apennines (italy): The 21 august 1962 irpinia multiple earthquake. *Tectono-*
756 *physics*, 691, 375–384.
- 757 Waldhauser, F., & Ellsworth, W. L. (2000). A double-difference earthquake location
758 algorithm: Method and application to the northern hayward fault, california.
759 *Bulletin of the seismological society of America*, 90(6), 1353–1368.
- 760 Wei, S., Avouac, J.-P., Hudnut, K. W., Donnellan, A., Parker, J. W., Graves, R. W.,
761 ... others (2015). The 2012 brawley swarm triggered by injection-induced
762 aseismic slip. *Earth and Planetary Science Letters*, 422, 115–125.
- 763 Westaway, R. (1987). The campania, southern italy, earthquakes of 1962 august 21.
764 *Geophysical Journal International*, 88(1), 1–24.
- 765 Wiemer, S. (2001). A software package to analyze seismicity: Zmap. *Seismological*
766 *Research Letters*, 72(3), 373–382.